Modeling of Electrochemical Cells:
Proton Exchange Membrane Fuel Cells
HYD7007 – 01

Lecture 11. Nonequilibrium Simulation of Polymers

Dept. of Chemical & Biomolecular Engineering
Yonsei University
Spring, 2011

Prof. David Keffer
dkeffer@utk.edu

Lecture Outline

- Atomistic simulations
  - method
  - visualization
  - rheological properties
  - structural properties
  - optical properties
  - flow-induced crystallization
  - frequency analysis
  - entanglement analysis
- Coarse-grained simulations
  - mesoscale models
  - continuum-scale viscoelastic models
  - Finite Element Modeling

Motivation

Polymers and other complex fluids have a molecular-level configuration that is a function of thermodynamic state.

The configuration is also a function of the presence of a nonequilibrium field, such as a flow field or an electric field.

Changes in molecular-level configuration due to the presence of a nonequilibrium field change macroscopic properties. The most common example of this is the shear-thinning behavior of fluids, where a macroscopic property, the shear viscosity, becomes smaller, as the shear rate increases, because of changes in the molecular configuration of the polymer.

Many fields are present in a proton exchange membrane. There is an electric field but there are also stresses due to the inhomogeneous distribution of water through-out the membrane and the movement of ions and water through the membrane. If we want to understand how the polymer responds to these fields, we need to be able to simulate polymers under nonequilibrium conditions.

MD simulations in Rheology:
Studies of nonequilibrium physical systems

➢ Equilibrium MD simulations for systems near equilibrium using nonequilibrium thermodynamics, *i.e.*, Onsager's reciprocal and Green-Kubo theorems

➢ Nonequilibrium MD (NEMD) simulations for general nonequilibrium systems, *i.e.*, flowing systems such as shear flow and elongational flow

<u>simple shear flow</u>

$$\nabla \mathbf{u} = \begin{bmatrix} 0 & \dot{\gamma} & 0 \\ 0 & 0 & 0 \\ 0 & 0 & 0 \end{bmatrix}$$

<u>elongational flows</u>

$$\nabla \mathbf{u} = \begin{bmatrix} \dot{\varepsilon}_{xx} & 0 & 0 \\ 0 & \dot{\varepsilon}_{yy} & 0 \\ 0 & 0 & \dot{\varepsilon}_{zz} \end{bmatrix}$$

NEMD algorithms

❑ Boundary-driven algorithm for shear flow

[A. W. Lees and S. F. Edwards, J. Phys. C **5**, 1921 (1972)]

❑ Field-driven algorithms

• DOLLS tensor algorithm

[W. G. Hoover et al., Phys. Rev. A **22**, 1690 (1980)]

• SLLOD algorithm

[D. J. Evans and G. P. Morriss, Phys. Rev. A **30**, 1528 (1984)]
[D. J. Evans and G. P. Morriss, *Statistical Mechanics of Nonequilibrium Liquids* (Academic Press, New York, 1990)]

• Proper SLLOD (*p*-SLLOD) algorithm

[M. E. Tuckerman et al., J. Chem. Phys. **106**, 5615 (1997)]
[B. J. Edwards and M. Dressler, J. Non-Newtonian Fluid Mech. **96**, 163 (2001)]
[C. Baig, B. J. Edwards, D. J. Keffer, and H. D. Cochran, J. Chem. Phys., **122**, 114103 (2005)]
[B. J. Edwards, C. Baig, and D. J. Keffer, *J. Chem Phys.* **124** 194104 (2006)]

Canonical (*NVT*) NEMD Simulations of PEF

- materials
  short-chain alkanes ($C_{10}H_{22}$, $C_{16}H_{34}$, and $C_{24}H_{50}$)
  polyethylene melts ($C_{50}H_{102}$, $C_{78}H_{158}$, and $C_{128}H_{258}$)

- Potential model
  Siepmann-Karaboni-Smit (SKS) united-atom model,
  except replacing a rigid bond by a flexible bond with
  harmonic potential

- Elongation rate

  $$0.0005 \leq \dot{\varepsilon}(m\sigma^2/\varepsilon)^{1/2} \leq 1.0.$$

Baig, C., Edwards, B.J., Keffer, D.J., Cochran, H.D., J. Chem. Phys., **122** (2005).
Baig, C., Edwards, B.J., Keffer, D.J., Cochran, H.D., Harmandaris, V.A., *J. Chem Phys.* **124** (2006).

YONSEI UNIVERSITY

Potential model

□ **Siepmann-Karaboni-Smit (SKS) united-atom model**

□ **Rigid bond between adjacent atoms → Harmonic potential function**

Non-bonded interactions

$$V_{LJ}(r) = 4\varepsilon_{ij}\left[\left(\frac{\sigma_{ij}}{r}\right)^{12} - \left(\frac{\sigma_{ij}}{r}\right)^{6}\right]$$

Bond-stretching interaction

$$V_{str}(l) = \frac{1}{2}k_{str}\left(l - l_{eq}\right)^2$$

Bond-torsional interaction

$$V_{tor}(\phi) = \sum_{m=0}^{3} a_m \left(\cos\phi\right)^m$$

Bond-bending interaction

$$V_{ben}(\theta) = \frac{1}{2}k_{ben}\left(\theta - \theta_{eq}\right)^2$$

Z-code

[Martin Kröger, Computer Physics Communications 168, 2005, 209-232]

☐ Identify entanglements and quantify entanglement statistics in polyethylene melts.
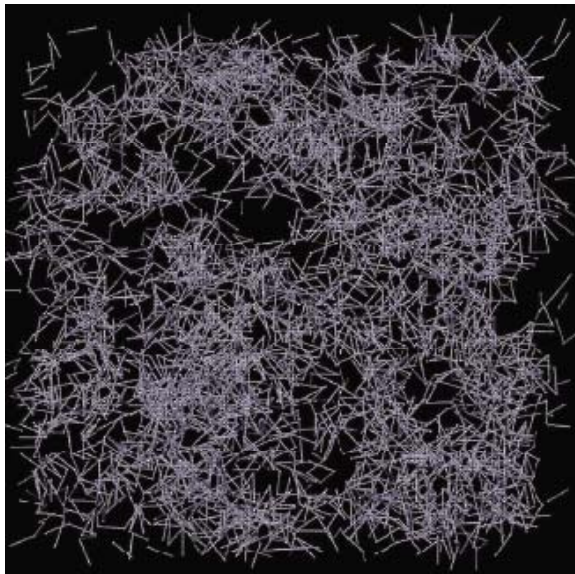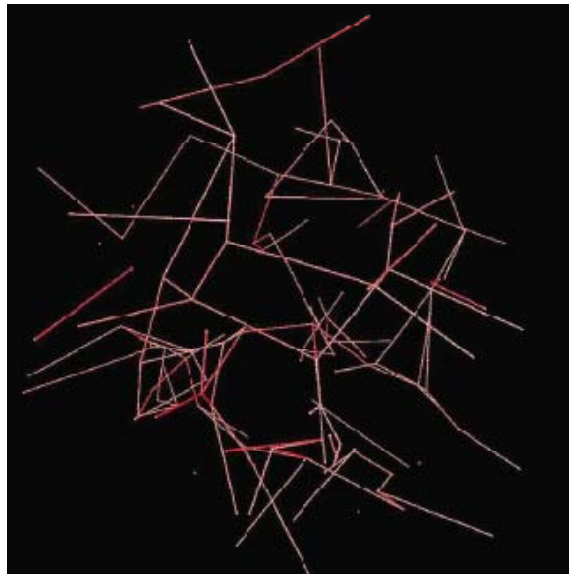
Original chains   Primitive path   Single chain with 2000 beads and 5000 obstacles in 2D

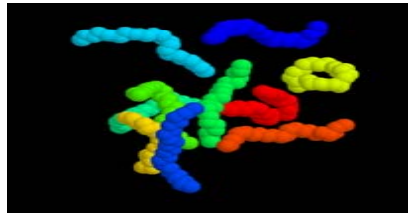Polymer melt with 10 chains of 500 beads in 3D
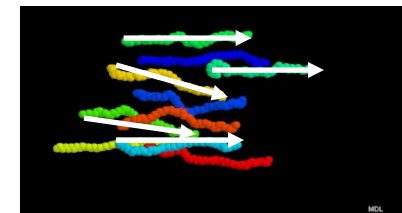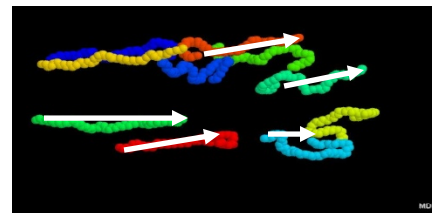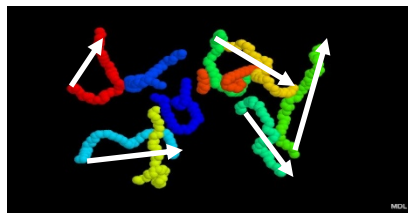
Visualization

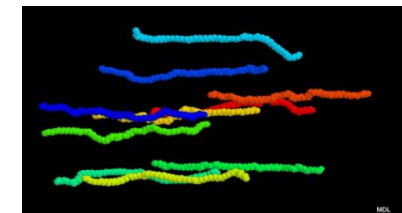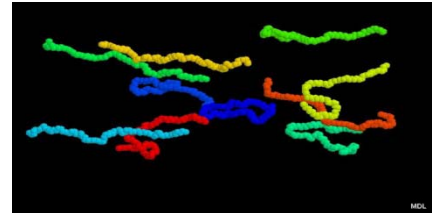|	Equilibrium	Shear ($\dot{\gamma}^* = 0.8$)	Elongation ($\dot{\varepsilon}^* = 0.2$)
Atomistic			
Primitive path			
Atomistic			
Primitive path			

Kim, J.M., Edwards, B.J.,Keffer, D.J., *Mol. Graph. & Mod.* **26**(7) 2008 pp. 1046-1056.
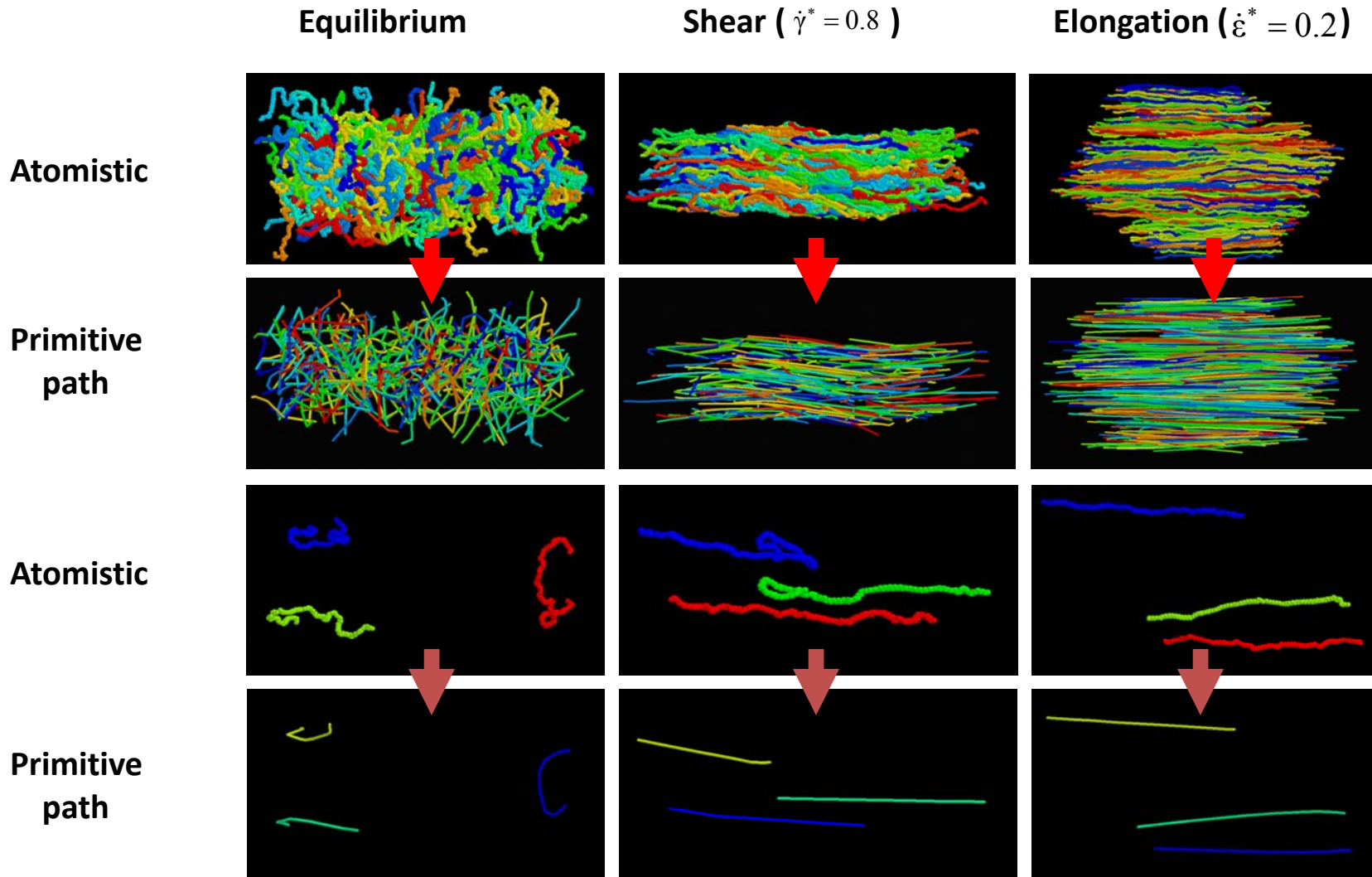
Visualization

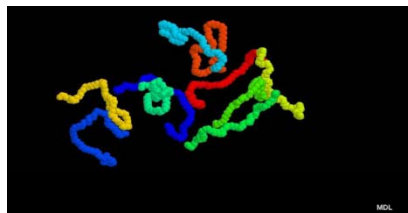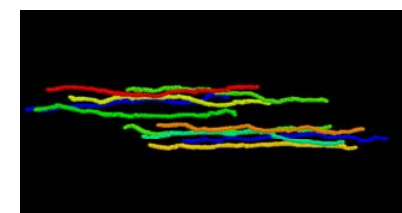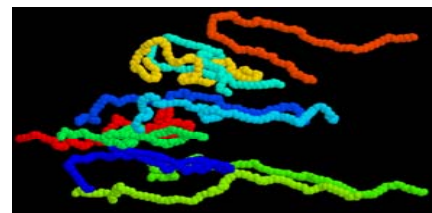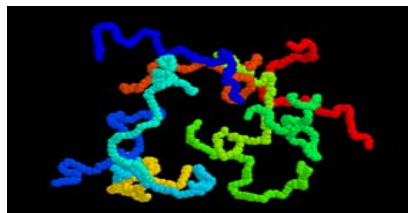| | Equilibrium | Shear ($\dot{\gamma}^* = 0.8$) | Elongation ($\dot{\varepsilon}^* = 0.2$) |

$C_{24}H_{50}$
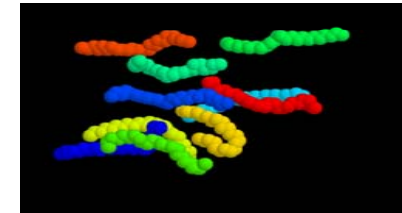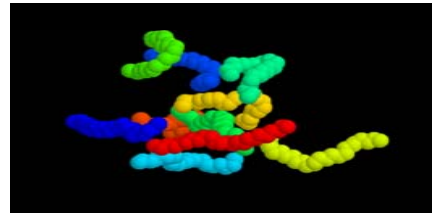
$C_{50}H_{102}$
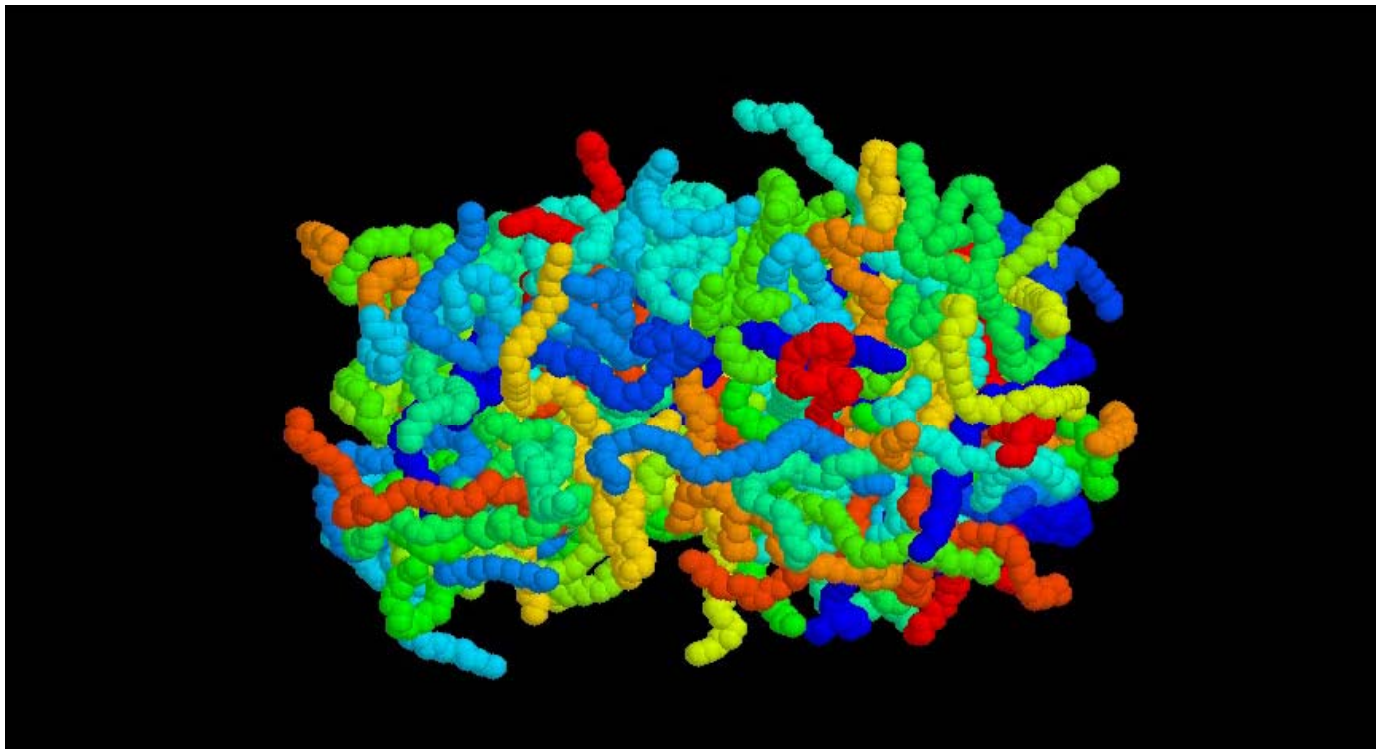
$C_{78}H_{158}$

$C_{128}H_{258}$

Visualization

$C_{50}H_{102}$ polyethylene melt at T=450K

☐ **Longest relaxation time (Rouse time) = 500 ps**

☐ **Real running time ≈ 70 ps**

Equilibrium

Visualization
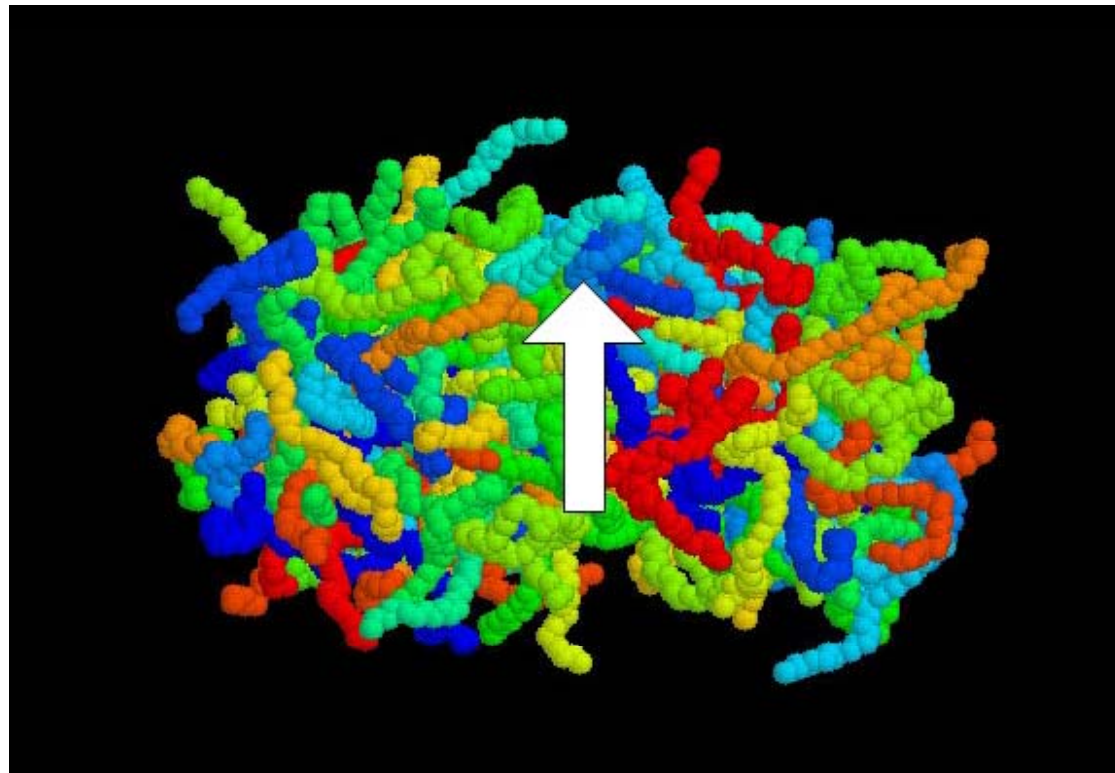
$C_{50}H_{102}$ polyethylene melt at T=450K (LEBC)

□ Longest relaxation time (Rouse time) = 500 ps

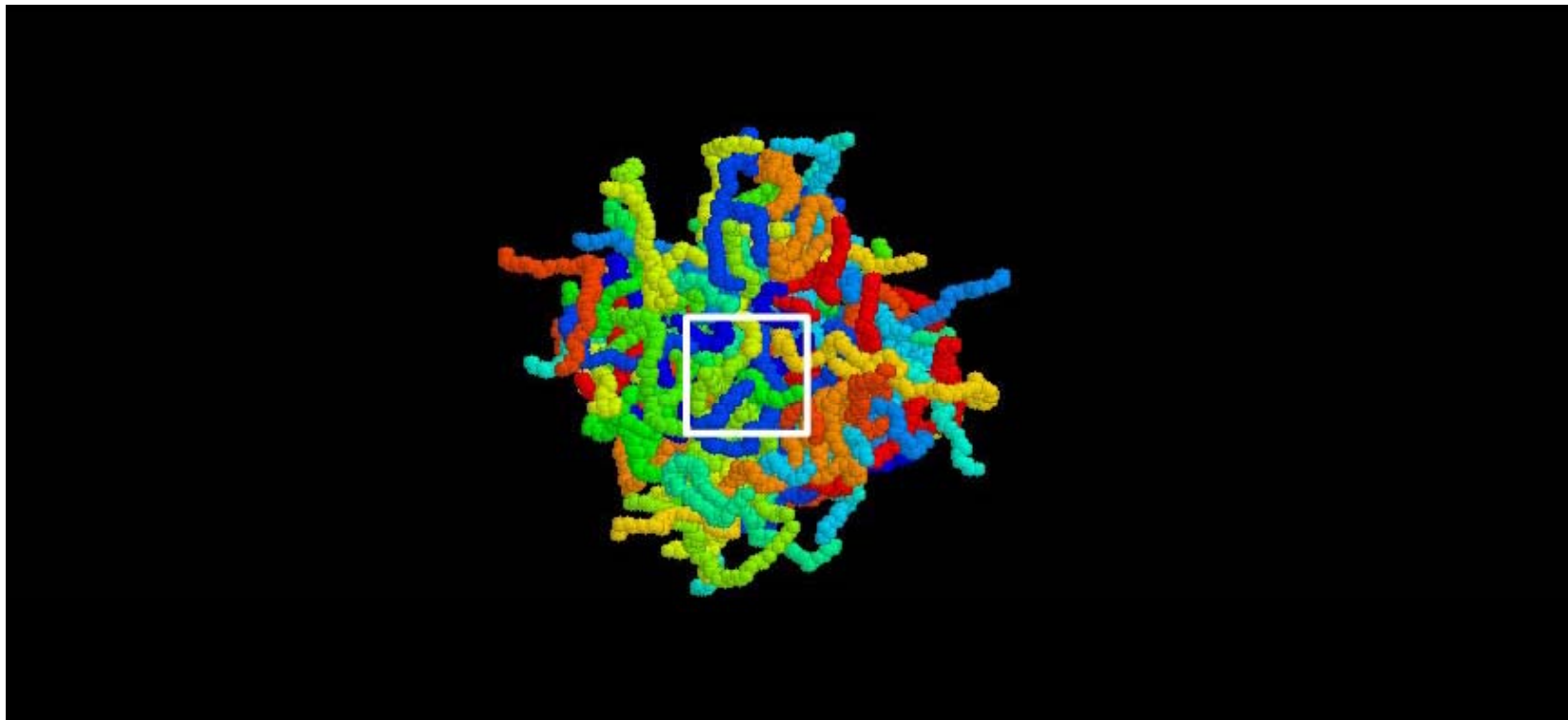□ Real running time ≈ 40 ps (Total ≈ 2350 ps)

Simple Shear

Visualization

$C_{50}H_{102}$ polyethylene melt at T=450K (KRBC)

□ Longest relaxation time (Rouse time) = 500 ps

□ Real running time ≈ 35 ps (Total ≈ 1800 ps)
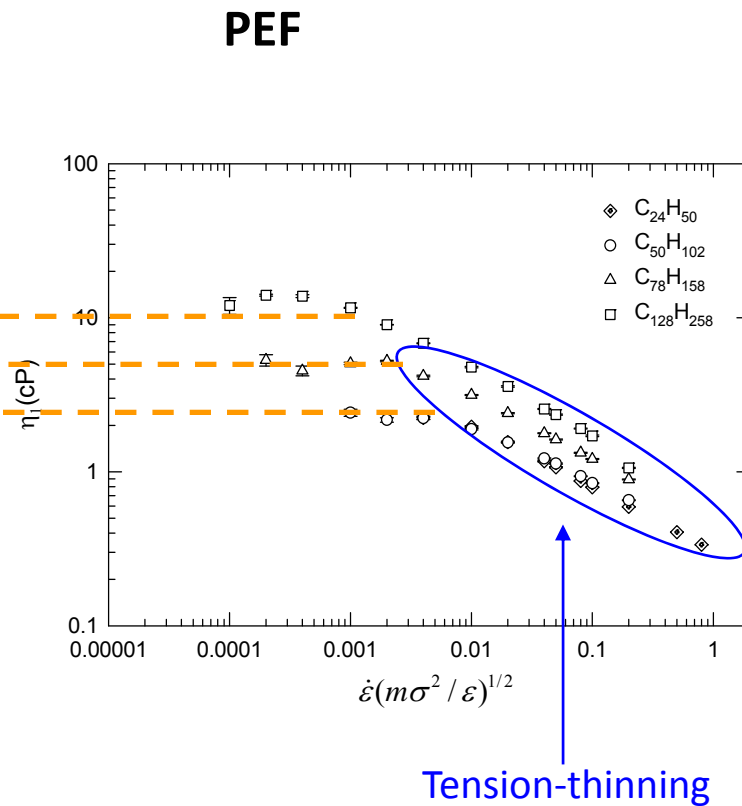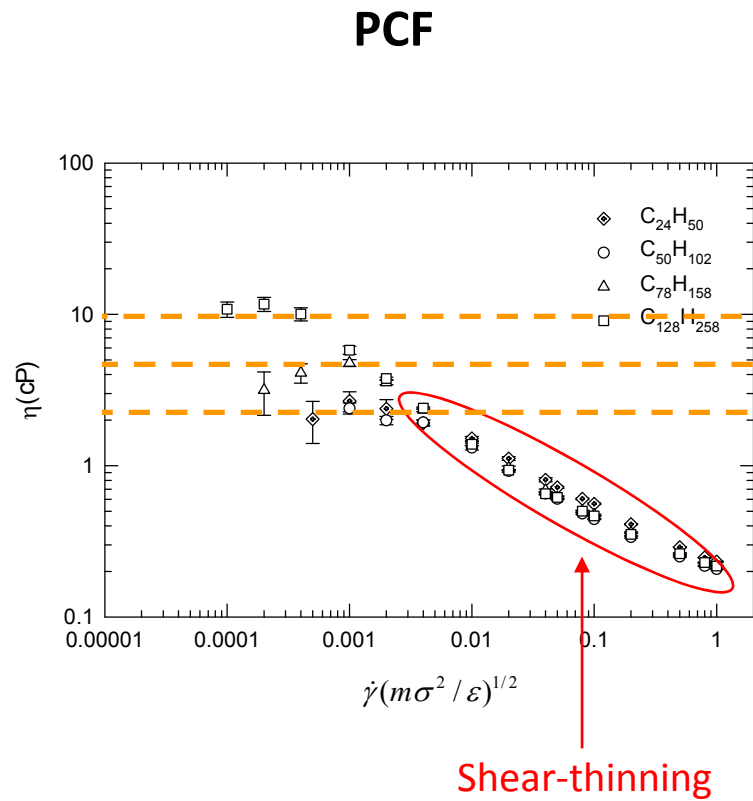
planar elongational flow

Viscosity

Viscosity

□ **Power law:** $\eta \sim \dot{\gamma}^b$ **(b = -0.34 ~ -0.46)**

PCF

PEF

Shear-thinning

Tension-thinning

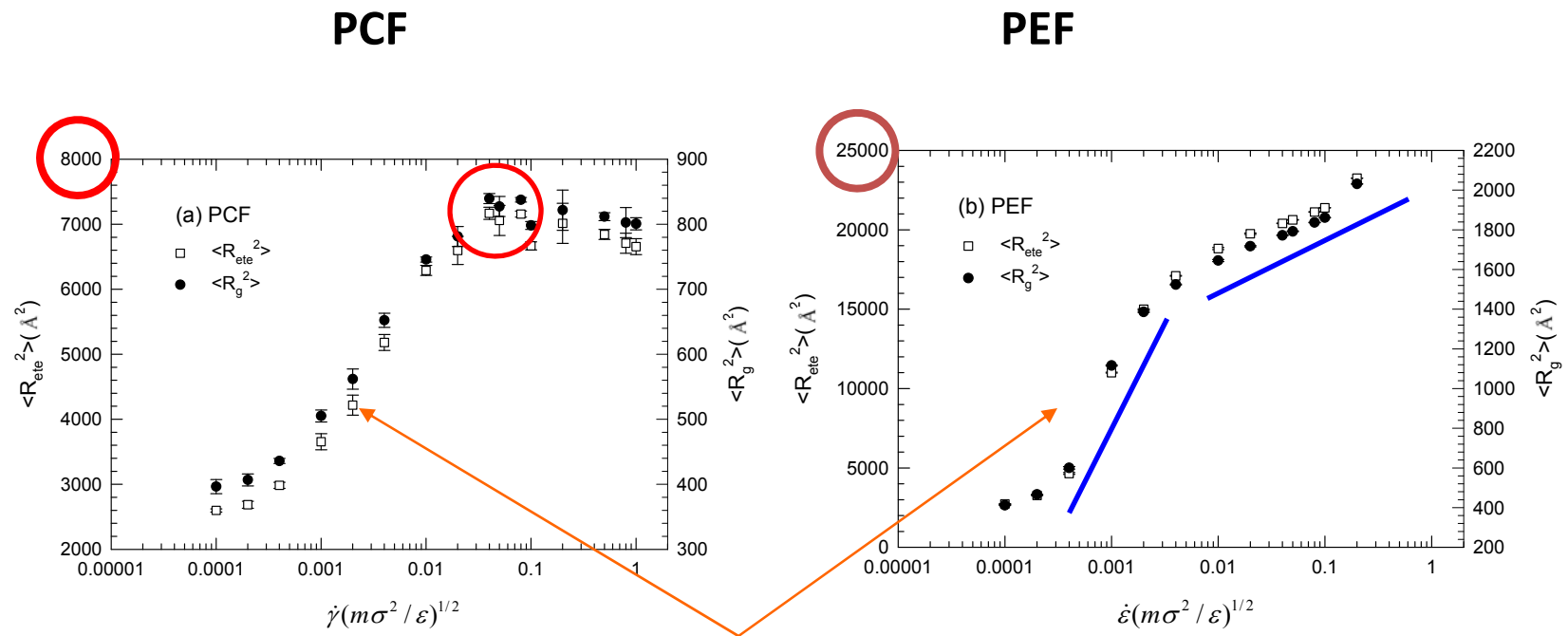Baig, C., Edwards, B.J., Keffer, D.J., Cochran, H.D., J. Chem. Phys., **122** (2005).
Baig, C., Edwards, B.J., Keffer, D.J., Cochran, H.D., Harmandaris, V.A., *J. Chem Phys.* **124** (2006).

Structural Properties

Mean square end-to-end distance and mean square chain radius of gyration

☐ **Fully-stretched length (R_{max}) for $C_{128}H_{258}$ = 164 Å**

☐ **R_{max}^2 = 26896 Å²**

PCF   PEF

Chain alignment & extension

$$\Delta \mathbf{n} = C \Delta \sigma$$

The deviatoric part of the refractive index tensor

$$\Delta \mathbf{n} = \mathbf{n} - \frac{1}{3} tr(\mathbf{n})\mathbf{I}$$

and the deviatoric part of the Cauchy stress tensor

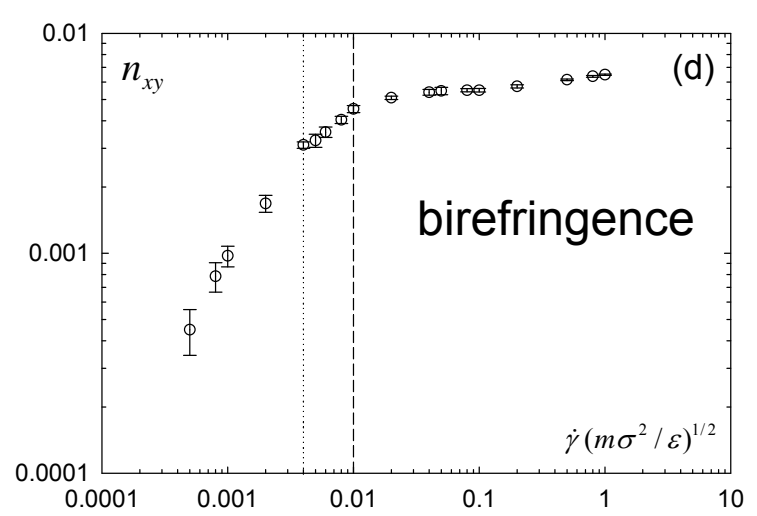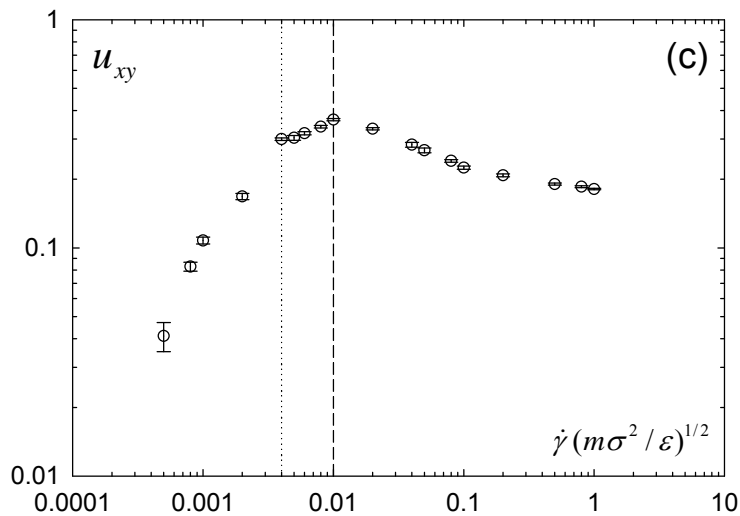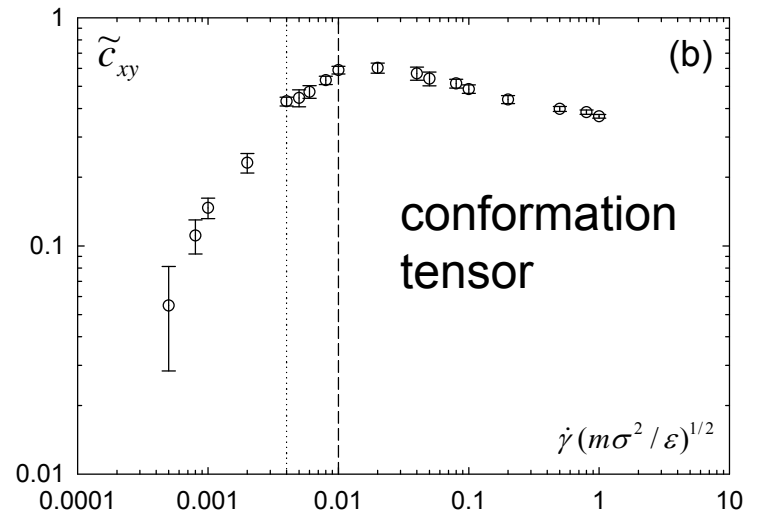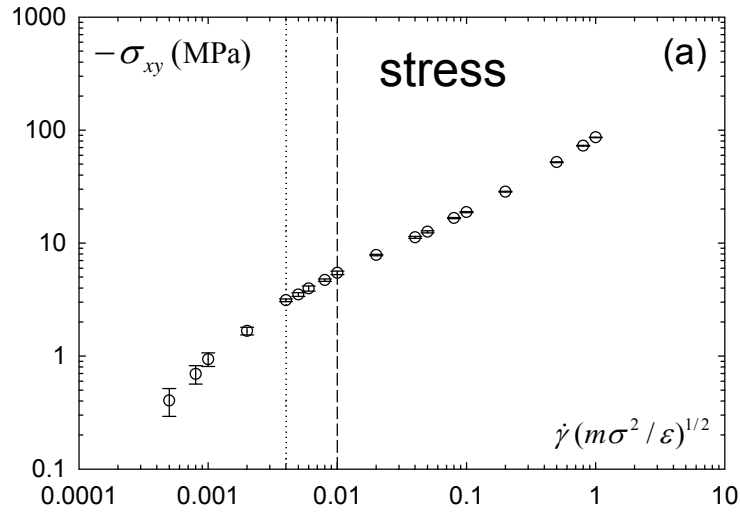$$\Delta \sigma = \sigma - \frac{1}{3} tr(\sigma)\mathbf{I}$$

are linearly proportional.

C is the stress-optical coefficient.

As a result, optical measurements can probe the state of stress in a material.

The Stress Optical Rule

Measure mechanical, structural and optical properties.

Baig, C., Edwards, B.J., Keffer, D.J., *Rheologica Acta.* **46** 2007 pp. 1171-1186.
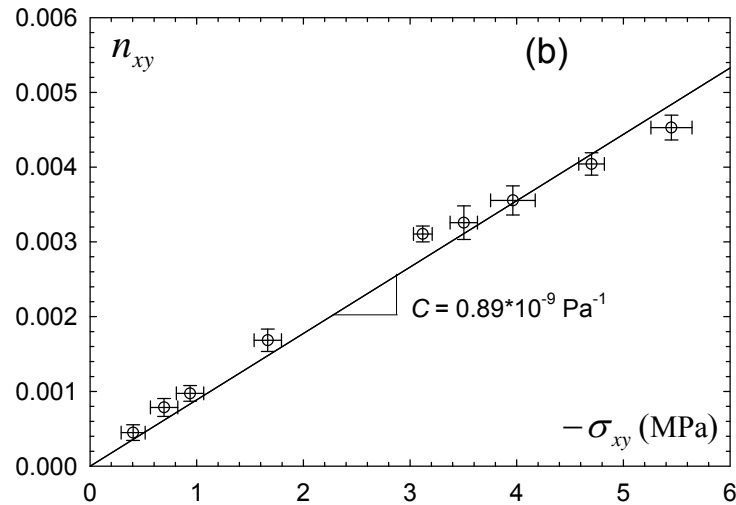
$$C = \begin{cases} 1.13 \pm 0.4 \times 10^{-9} \text{ Pa}^{-1} \text{ in this study} \\ 2.35 \times 10^{-9} \text{ Pa}^{-1} \text{ for HDPE at T} = 423\text{K} \end{cases}$$

[Janeschitz-Kriegl 1983]
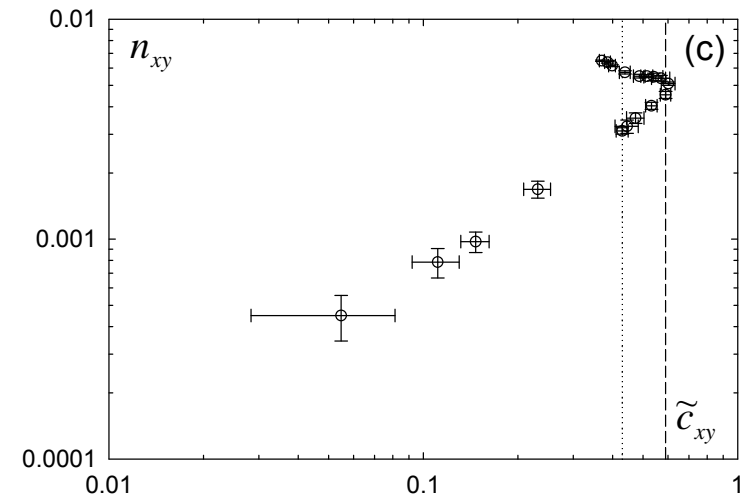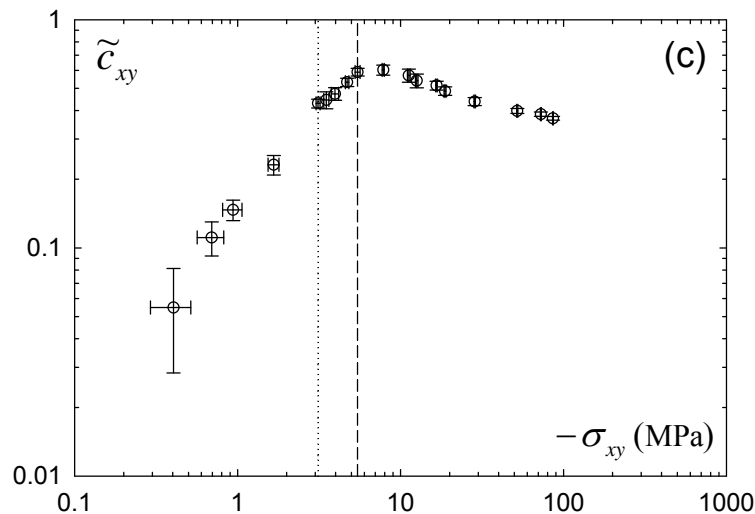
The customary view that the SOR breaks down due to the saturation of chain extension and orientation was demonstrated to be incorrect under shear.
The breakdown point of the SOR occurred at 27 % of the full extension and 23° of the birefringence orientation angle (≈12 ° at high shear rates)

Flow-Induced Crystallization

We have shown that a flow field can change the molecular-level configuration of the polymer. It can be so dramatic as to cause crystallization above the thermodynamic melt temperature.

We know the structure of polyethylene as a melt in the absence of a flow field.

The state point was chosen the same as in the experiment case (n-eicosane , T = 315K and ρ = 0.81 g/cc), and the experimental scattering data were taken from literature (*).
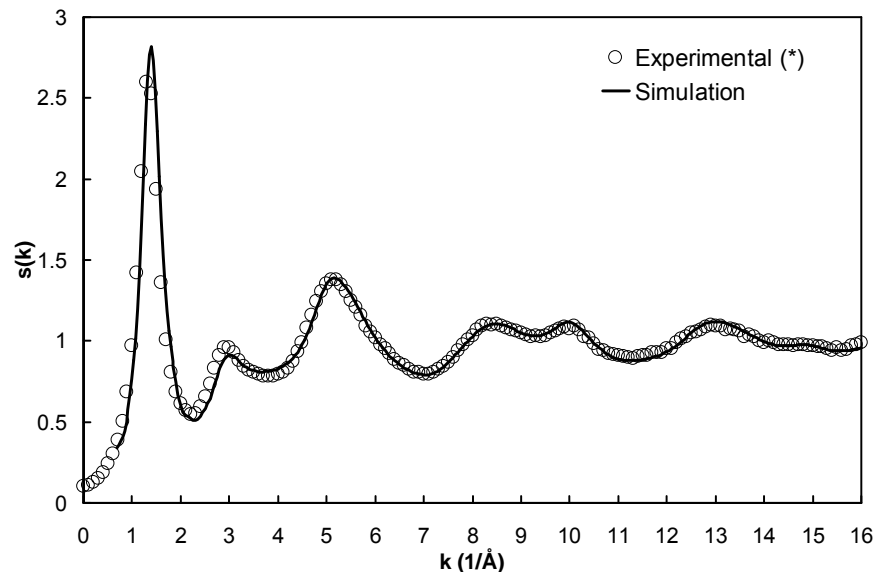
Ionescu, T.C., et al.,. *Physical Review Letters*, 2006. **96**(3).
(*) A. Habenschuss and A.H. Narten, *J. Chem. Phys.*, **92**, 5692 (1990)

Flow-Induced Crystallization

One can see by comparison of the simulated structures for the quiescent (flow free) melt and the polymer under an elongational flow, that there are systematic changes in the structure.
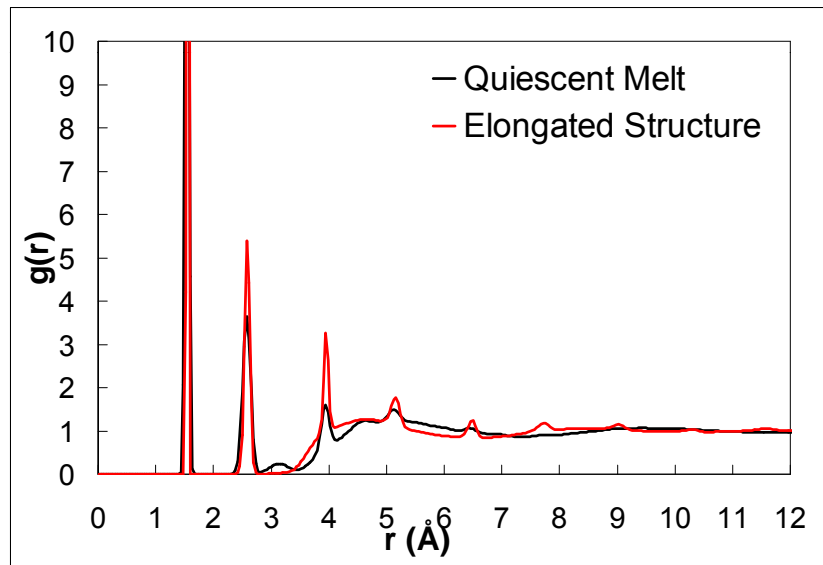
pair correlation function
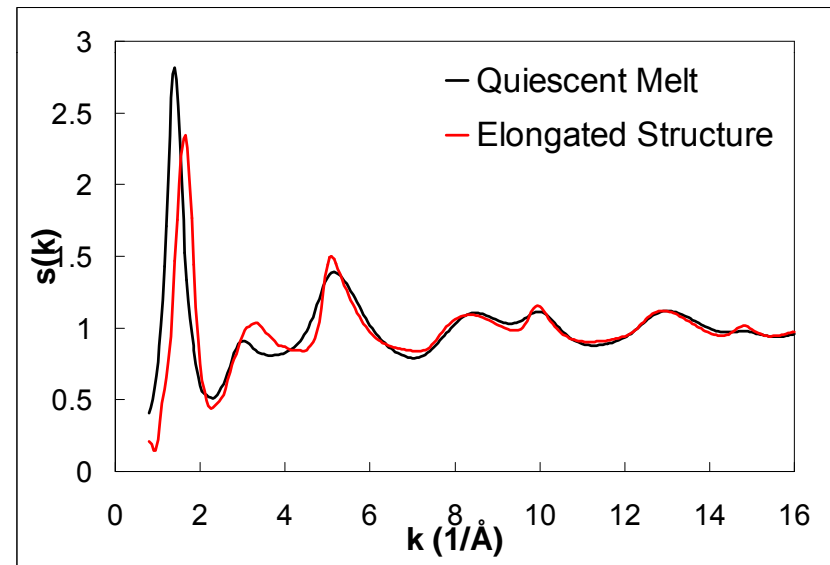
fourier transform

Ionescu, T.C., et al.,. *Physical Review Letters*, 2006. **96**(3).
(*) A. Habenschuss and A.H. Narten, *J. Chem. Phys.*, **92**, 5692 (1990)

Flow-Induced Crystallization

While experimental data is not available for flow-induced crystals, is it available for crystals formed by lowering the temperature. We therefore compare the structure under elongational flow from simulation with the structure of a thermally induced crystal from experiment.

- Identify two regions:
  - Inter-molecular region ($k<6Å^{-1}$), where sharp Bragg peaks are present
  - Intra-molecular region ($k>6Å^{-1}$), where the agreement with simulation is excellent
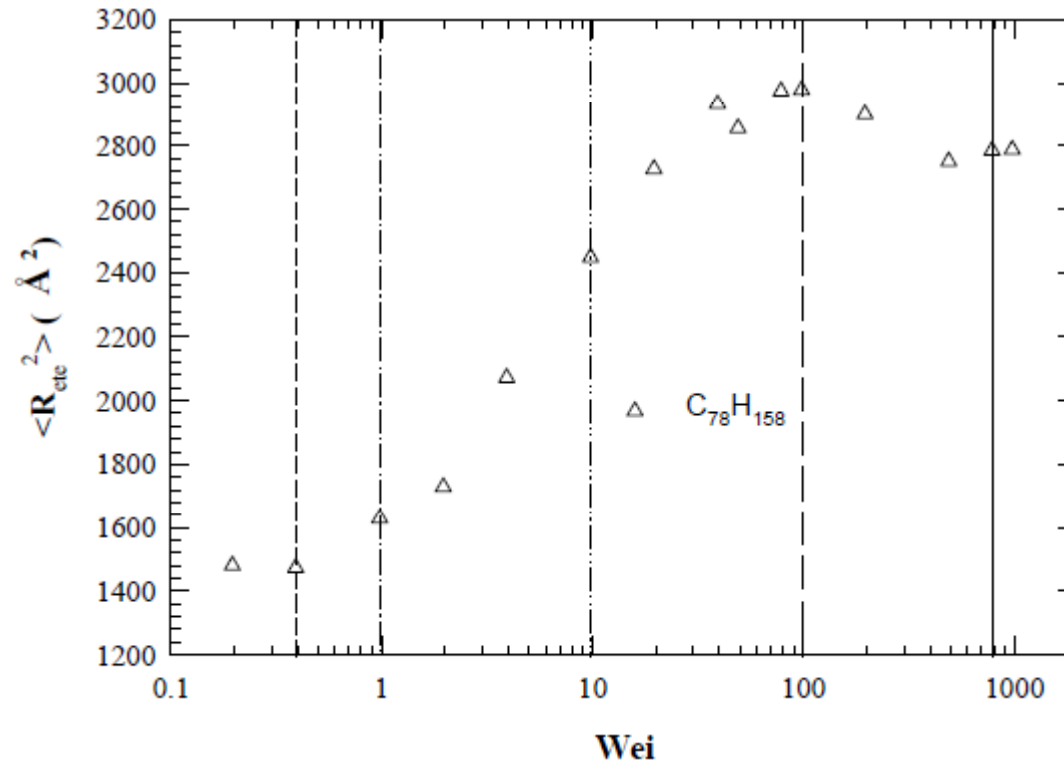
In shear flow, we know that as the shear rate increases (characterized here by the dimensionless Weisenberg number), the average end-to-end distance in a chain changes.

Kim, J.M., Edwards, B.J., Khomami, B., Keffer, D.J., *Phys. Lett. A* **373**(7) 2009 pp. 769-772.

Single Chain Dynamics
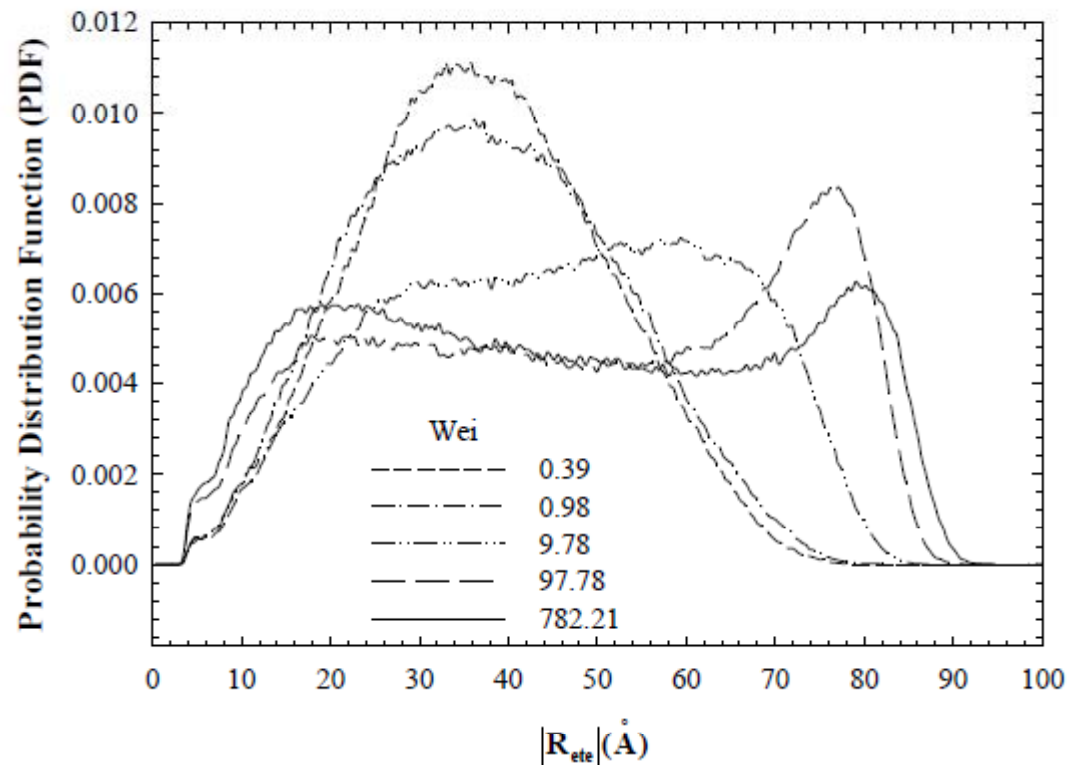
It's not just the average value of the end-to-end distance that changes, but the distribution changes.

Kim, J.M., Edwards, B.J., Khomami, B., Keffer, D.J., *Phys. Lett. A* **373**(7) 2009 pp. 769-772.

Single Chain Dynamics
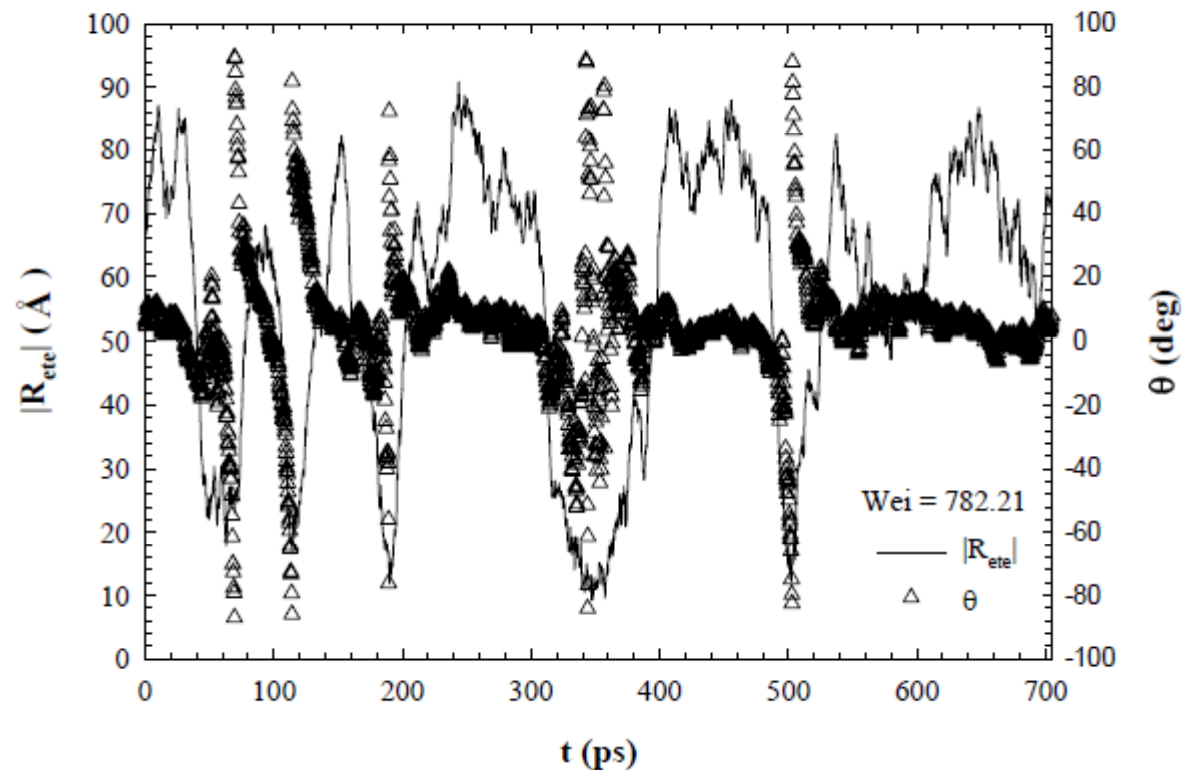
These changes in configuration can be understood by following individual chain dynamics. In shear flow, there is a vorticity present, which induces chain tumbling.

One can Fourier transform this kind of data to extract frequencies of chain rotation.

Kim, J.M., Edwards, B.J., Khomami, B., Keffer, D.J., *Phys. Lett. A* **373**(7) 2009 pp. 769-772.

Single Chain Dynamics
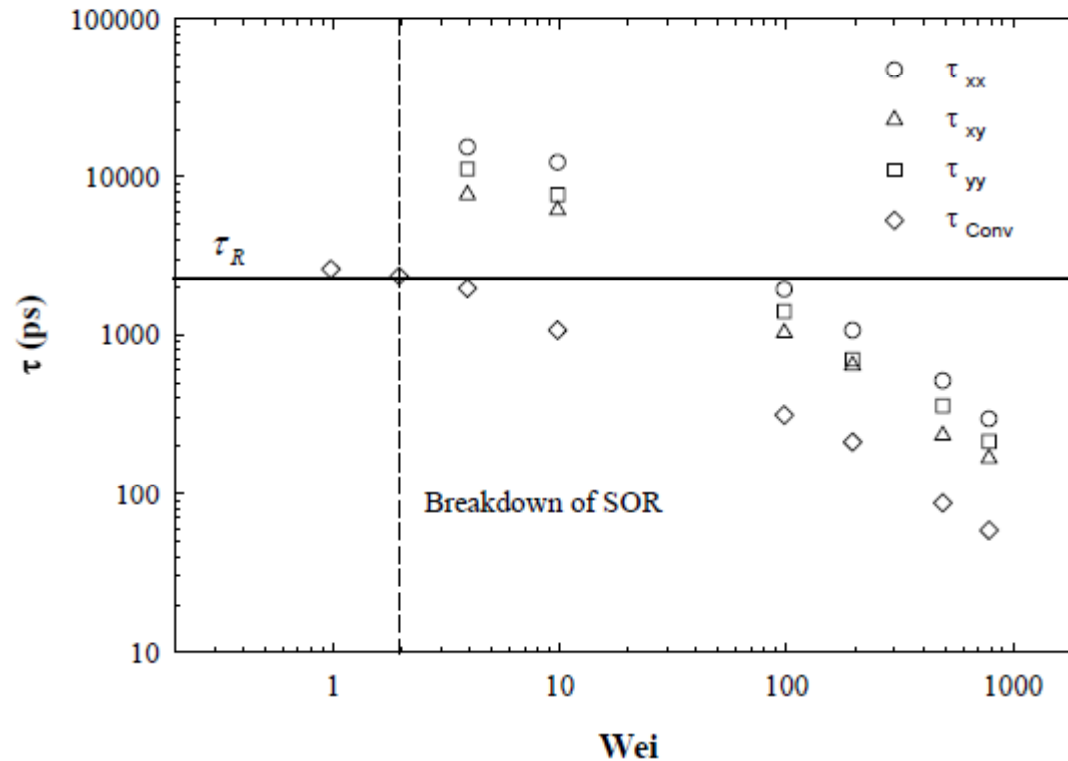
The rotational period of chains is a function of shear rate. At low shear rate, there is an equilibrium value, the Rouse time. As shear rate increases, the rotational period of chains decreases.

Kim, J.M., Edwards, B.J., Khomami, B., Keffer, D.J., *Phys. Lett. A* **373**(7) 2009 pp. 769-772.

Entanglement Analysis
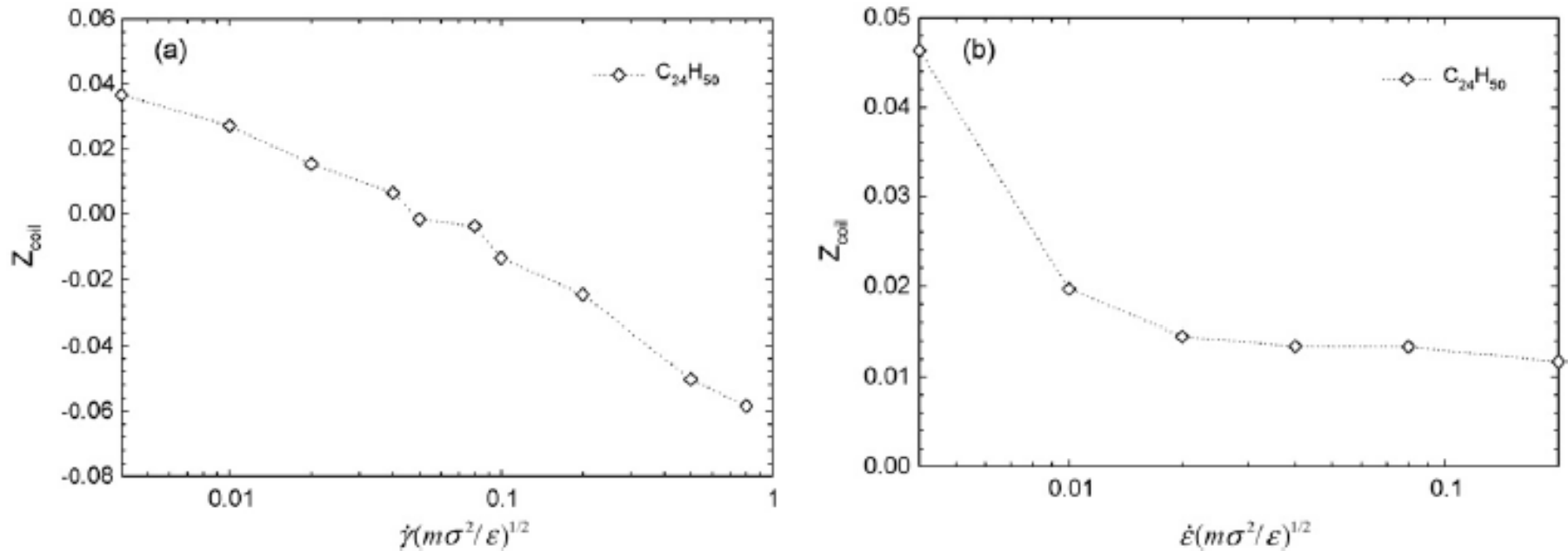
Fig. 13. 'Number of entanglements' Z_{coil} (assuming equilibrium statistics) vs. strain rate for $C_{24}H_{50}$.

Flow fields (shear flow (left), elongational flow (right)) also can cause the number of entanglements per chain to decrease, i.e. the chains become less entangled at high flow rates, contributing to a reduction in viscosity, e.g. shear-thinning behavior.

Kim, J.M., Keffer, D.J., Kröger, M., Edwards, B.J., *J. Non-Newtonian Fluid Mech.* **152**(1-3) 2008 pp. 168-183.

Lecture Outline

- Atomistic simulations
  - method
  - visualization
  - rheological properties
  - structural properties
  - optical properties
  - flow-induced crystallization
  - frequency analysis
  - entanglement analysis
- Coarse-grained simulations
  - mesoscale models
  - continuum-scale viscoelastic models
  - Finite Element Modeling

Mesoscale Models

Brownian Dynamics (BD) simulations of mesoscale models such as bead-rod chains are simpler and computationally less demanding.
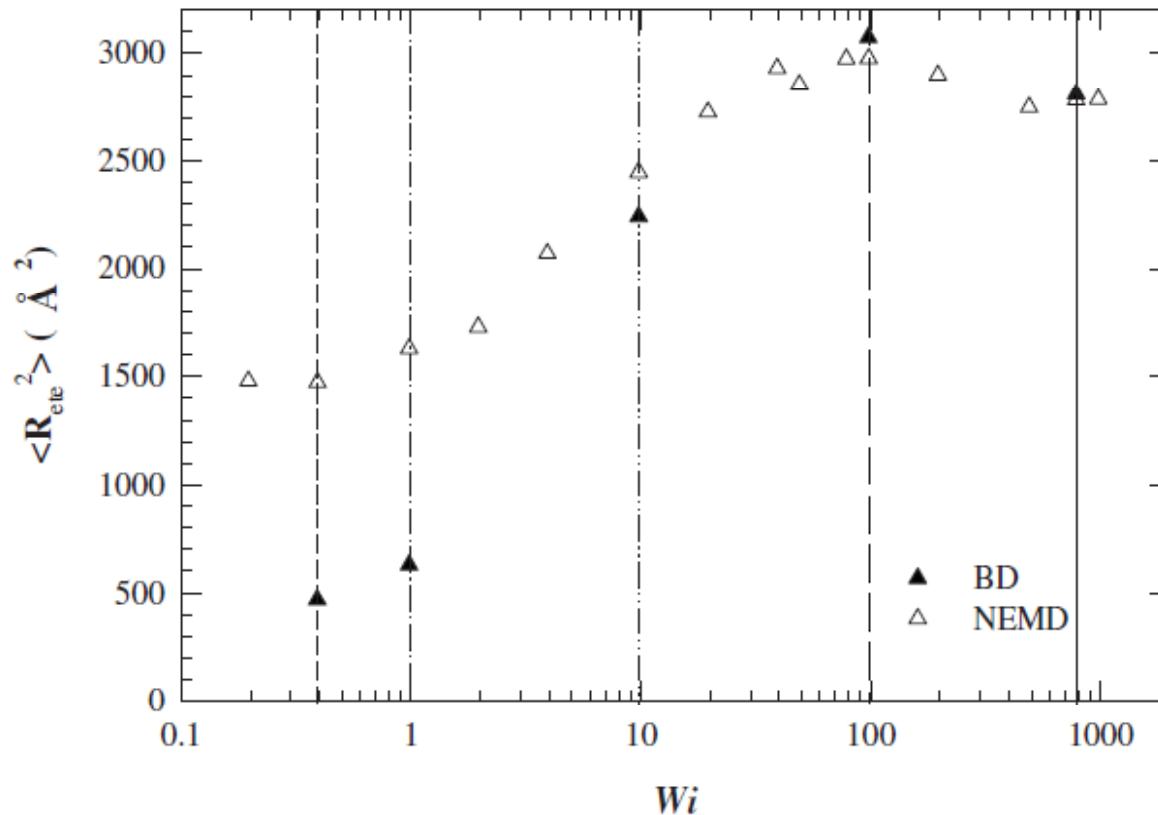
FIG. 2. The mean-square chain end-to-end distance, $\langle R_{ete}^2 \rangle$, for $C_{78}H_{158}$ as a function of Wi from the atomistic NEMD (open symbols) and BD (filled symbols) simulations.

The comparison between BD mesocale and MD atomistic simulations is reasonably good.
Where they do disagree, the explanation is known.

Mesoscale Models
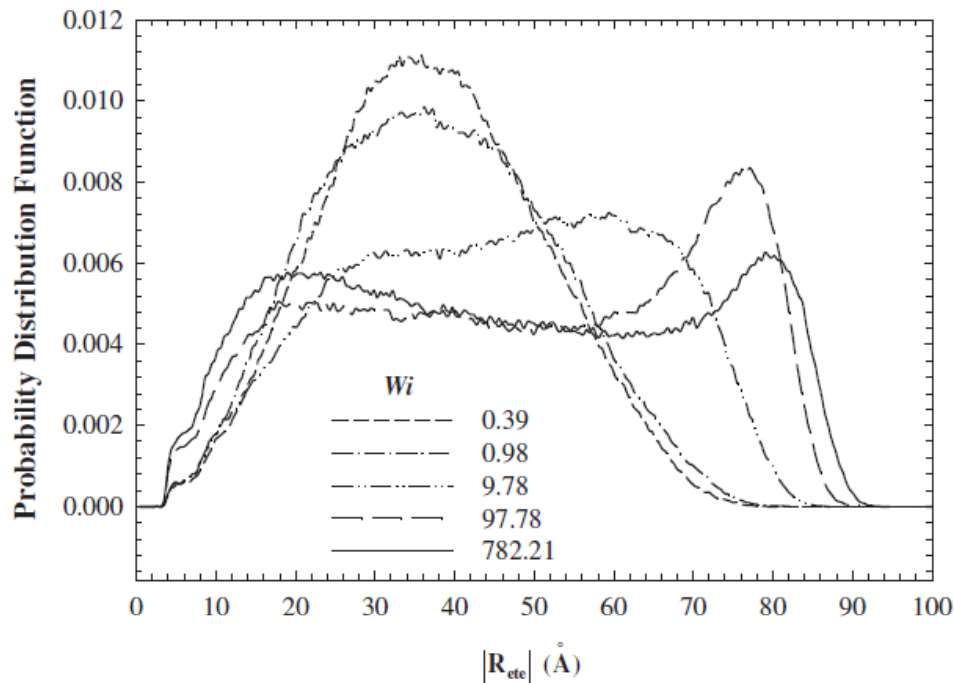
BD mesoscale simulation

MD atomistic simulation

The MD and BD simulations show a similar departure from an equilibrium distribution of structures in the presence of the flow field.

Continuum Viscoelastic Models

FIG. 1. Comparison between the model predictions and simulation data for the conformation tensor versus shear rate under PCF: (a) $\tilde{c}_{xy}$, (b) $\tilde{c}_{xx}$, (c) $\tilde{c}_{yy}$, and (d) $\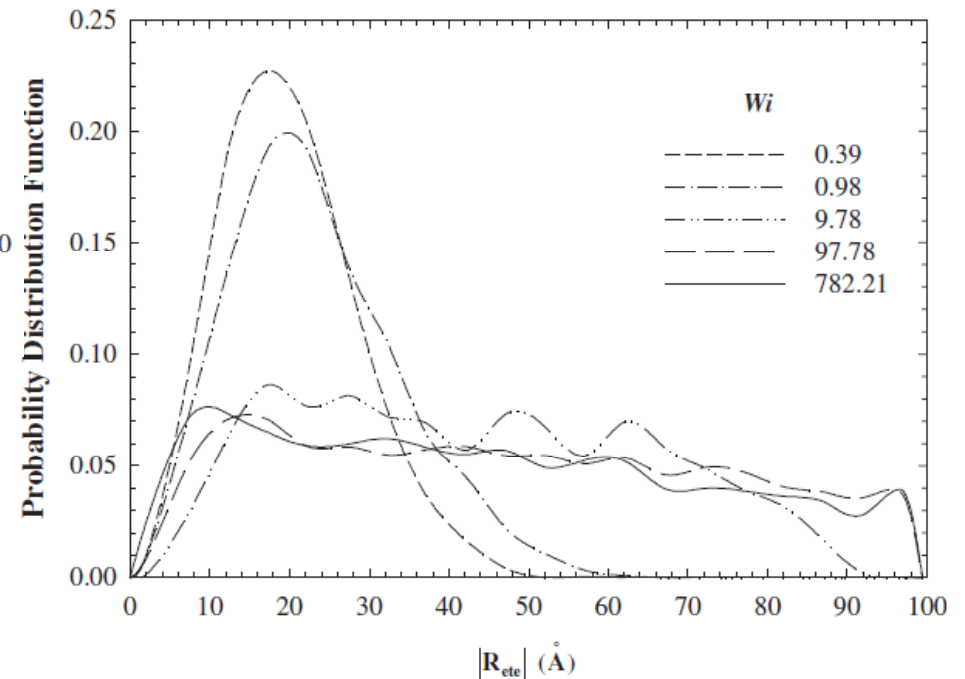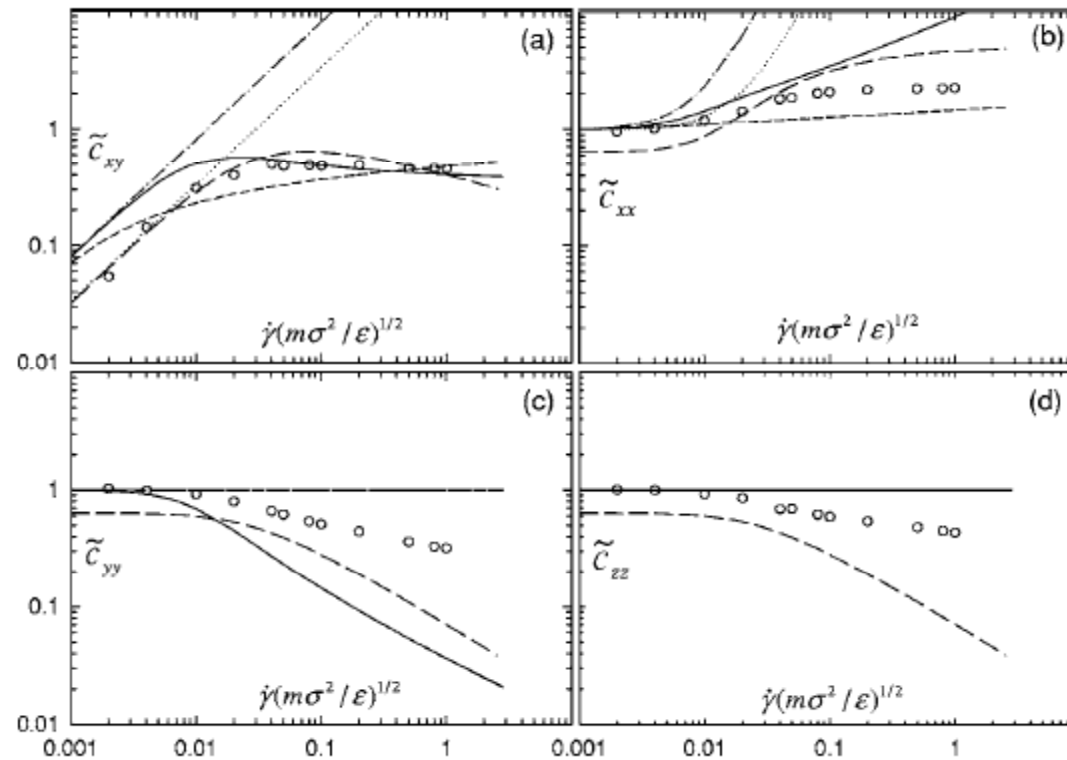tilde{c}_{zz}$. The circles and lines, respectively, represent the simulation data and the model predictions: the UCM model (the dashed-dotted lines), the Rouse model (the dotted lines), the EWM model (short-dashed lines), the FENE-p model (long-dashed lines), and the Giesekus model (solid lines). Notice that (c) and (d) appear to have fewer lines due to the overlap between lines.

Constitutive equations for Non-Newtonian fluids account for structural changes in the configuration and can be fit to data from atomistic simulation.
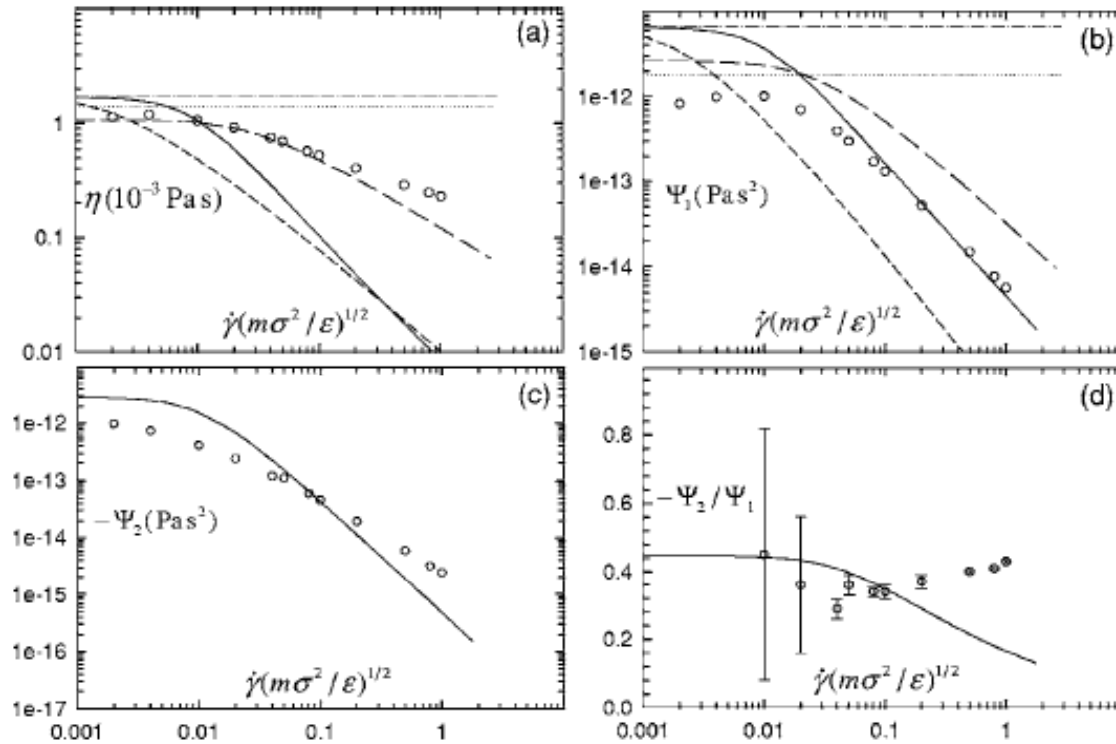
Baig, C., Jiang, B., Edwards, B.J., Keffer, D.J., Cochran, H.D., *J. Rheol.* **50**(5) 2006 pp. 625-640.

Continuum Viscoelastic Models

FIG. 2. Comparison between the model predictions and simulation data for the steady-state material functions in PCF: (a) Shear viscosity, (b) first normal stress coefficient, (c) second normal stress coefficient, and (d) the ratio of second to first normal stress coefficients. The symbols and lines represent the same quantities as in Fig. 1. Note that all models except the Giesekus predict a vanishing second normal stress coefficient.

These constitutive equations then provide material properties, such as the shear viscosity that can be used in continuum simulations.

Baig, C., Jiang, B., Edwards, B.J., Keffer, D.J., Cochran, H.D., *J. Rheol.* **50**(5) 2006 pp. 625-640.

Finite Element Method

- Temperature Distribution in Elongational flow of HDPE for different strain rates

$$\dot{\varepsilon} = 2s^{-1} \qquad \dot{\varepsilon} = 10s^{-1} \qquad \dot{\varepsilon} = 50s^{-1}$$
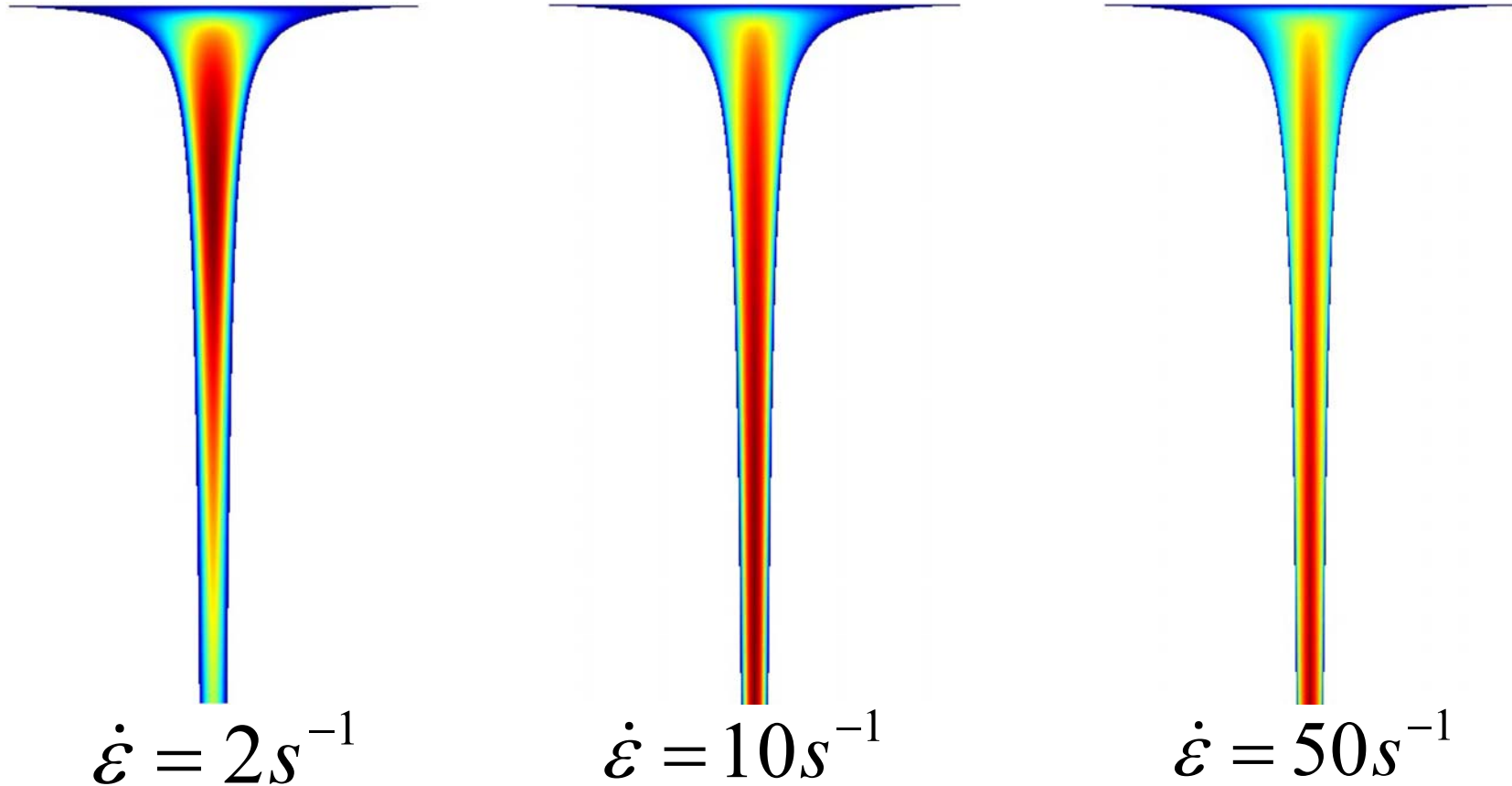
These flows involve strong chain reorientation. A viscoelastic model that accounts for chain reorientation is essential to describing these flows.
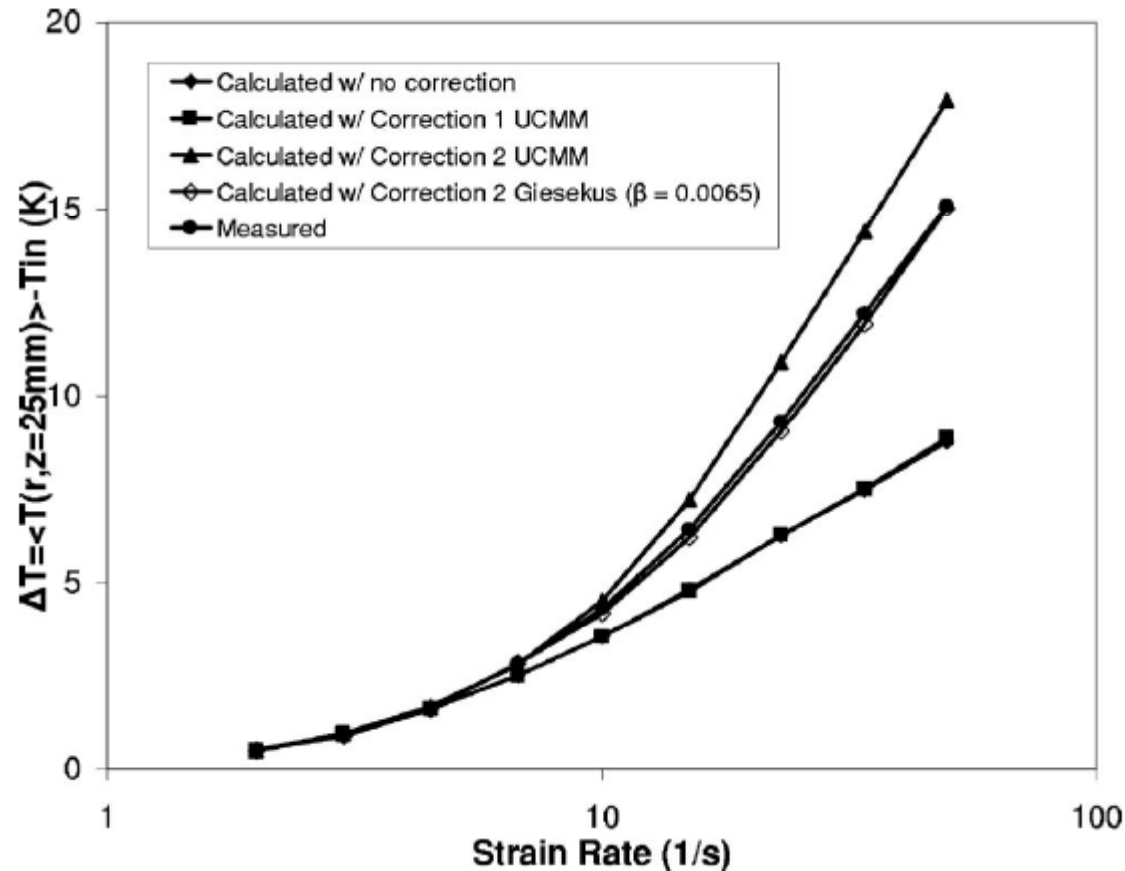
Ionescu, T.C., Edwards, B.J., Keffer, D.J., Mavrantzas, V. G., *J. Rheol.* **52**(1) 2008 pp. 105-140.

Finite Element Method

FIG. 14. Relative effects of correcting for the conformational part of the heat capacity (correction 1) and for the extra heat generation term (correction 2) in the calculated temperature profiles for the HDPE melt at T_{in} = 190 °C.

The temperature rise can only be accounted for by including heat generation due to conformational changes.

Ionescu, T.C., Edwards, B.J., Keffer, D.J., Mavrantzas, V. G., *J. Rheol.* **52**(1) 2008 pp. 105-140.

Conclusions:

- Nonequilibrium simulations are necessary to understand the configurational changes that complex fluids undergo in response to external fields.

- Atomistic simulations can be used to
  - visualize conformational changes
  - predict rheological, structural and optical properties
  - predict flow-induced crystallization
  - structural changes and chain dynamics can be understood in terms of molecular-level mechanisms seen in NEMD simulations

- Coarse-grained simulations
  - can be fit to results of results of atomistic simulations
  - can take the form of mesoscale models or
  - continuum-scale viscoelastic models
  - Finite Element Method (FEM) modeling of continuum systems using viscoelastic models based on atomistic NEMD data provides excellent description of observed experimental behavior.

- These NEMD simulations have been applied to flow field, but can also be applied to the combined electric and flow fields in fuel cells.

Acknowledgements

Chunggi Baig and Jun Mo Kim with Ruth, Joseph and David Keffer (2008).